CrystEngComm

Cite this: *CrystEngComm*, 2012, **14**, 4243–4246

www.rsc.org/crystengcomm

COMMUNICATION

Formation and nonlinear optical properties of carbon nanospindles from laser ablation

Shengliang Hu,*[ab] Yingge Dong,[b] Jinlong Yang,[bc] Jun Liu[a] and Shirui Cao[b]

Received 31st January 2012, Accepted 21st March 2012
DOI: 10.1039/c2ce25145k

Carbon nanospindles are synthesized by laser ablation of carbon black suspension. Their formation could be originated from the coalescence of small carbon nanocrystals because enough time and energy are provided at a long pulse width. At the same level of linear transmittance, carbon nanospindle suspension exhibits better nonlinear optical effects with a 532-nm laser beam than carbon black suspension. The possible mechanism for optical limiting is attributed to the nonlinear scattering from the micro-bubbles.

Laser ablation in liquid is known as an effective and green way for the fabrication of nanocrystals.[1–6] Generally, the short-pulse-width laser with a pulse width of several nanoseconds and power density of 10^9–10^{11} W cm^{-2} was employed.[2–6] This could provide high energy flux in a short time window to generate plasma and vapor. Under rapid cooling rates, plasma and vapor were condensed to form ultrafine nanoparticles.[7] Recently, Yang and co-workers reported a method of the electrical field assisted laser ablation in liquid.[2,6] By this technique, micro- and nanospindles were synthesized. In contrast, the lower temperature and different mechanism for forming nanocrystals could be obtained by using a long-pulse-width laser with a pulse width of several milliseconds and power density of 10^6–10^7 W cm^{-2}.[1,8–10] Employing such a laser, a variety of nanostructures, such as hollow nanoparticles, core-shell nanoparticles, and ordered arrays, were fabricated by Niu *et al.*[1] In their experiment, the laser pulse width was unchanged at 1 ms to allow for experimental comparison. In the present work, a longer pulse-width was selected and then short carbon nanospindles were formed by coalescence of small carbon nanocrystals under laser irradiation of carbon black suspension without any assistance.

Many carbon nanostructures, *e.g.* carbon black, carbon nanotube, graphene, and carbon onion, have been reported to have strong optical limiting (OL) effects in the nanosecond regime. It is generally believed that their OL effects arise from strong nonlinear scattering (NLS).[11–14] The OL effects from the suspensions of noble metal and semiconductor nanoparticles with several nanometers are majorly attributed to free-carrier absorption (FCA).[15–17] However, the FCA role will be replaced by the NLS effect with increasing particle size and aggregation of nanoparticles, thus resulting in the lower OL threshold.[16,17] Since recent achievements suggested that ultrafine carbon nanoparticles share the major characteristics of traditional semiconductor nanoparticles,[18] carbon nanospindles from coalescence of small carbon nanocrystals should have good OL properties based on the above consideration.

Furnace carbon black particles with an average 200 nm diameter were used as the precursor. They were mixed with water, and then the carbon black suspension in the water was irradiated by a Nd:YAG pulsed laser with power density of 6×10^6 W cm^{-2}. The laser beams were focused on the suspension surface with a spot diameter of 0.3 mm. The wavelength length, frequency, pulse width, and irradiation time were 1064 nm, 5 Hz, 8 ms and 2 h, respectively. Simultaneously, ultrasonics were employed to expedite the movement of carbon black particles during laser irradiation. The unreacted carbon blacks were removed by boiling in perchloric acid, and then the sample was obtained. The morphology and structure of the sample were characterized using an FEI Technai G2 F20 transmission electron microscope (TEM) with a field-emission electron gun and a Renishaw MKI-2000 laser Raman spectrometer at an excitation wavelength of 632.8 nm. The open-aperture Z-scan technique was used to measure the optical limiting responses of the sample. All experiments were performed with 6 ns Gaussian pulses from a Q-switched Nd:YAG laser. The laser was operated at the second harmonic, 532 nm, with a pulse repetition rate of 1 Hz. The beam was spatially filtered to remove higher-order modes and focused with a lens with a focal length of 20 cm. The scattered light was collected at 45° to the direct incident beam. For the OL experiments, all of the sample concentrations were adjusted to have the same linear transmittance of 81% at 532 nm in 5 mm quartz cells.

To compare the microstructures between carbon black and the obtained sample, their TEM images and the selected area electron diffraction (SAED) patterns are shown in Fig. 1, respectively. Carbon black particles are spherical (Fig. 1a) and show an amorphous structure (the inset of Fig. 1a). There are no detectable diffraction spots in Fig. 1c. In contrast, it can be seen from Fig. 1b

[a]*Key Laboratory of Instrumentation Science & Dynamic Measurement, Ministry of Education, Science and Technology on Electronic Test and Measurement Laboratory, Taiyuan 030051, P. R. China. E-mail: hsliang@yeah.net; Fax: 86 351 3559638; Tel: 86 351 3559638*
[b]*School of Material Science and Engineering, North University of China, Taiyuan 030051, P. R. China*
[c]*State Key Laboratory of New Ceramics and Fine Processing, Tsinghua University, Beijing 100084, P. R. China*

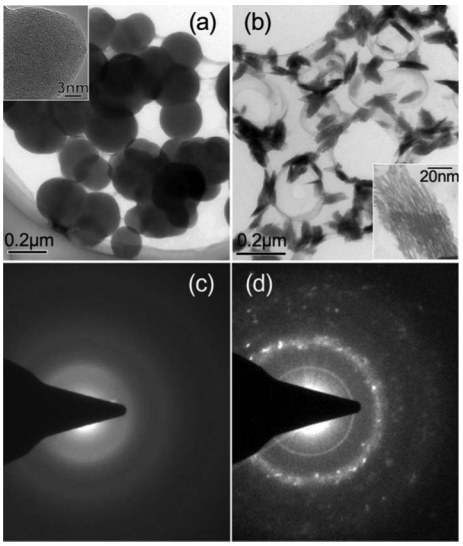

Fig. 1 TEM images and SAED patterns of carbon black particles (a), (c) and carbon nanospindles (b), (d), respectively. The insets of (a) and (b) are amplification images of carbon black and shuttle-like nanostructure.

that the well-dispersed carbon nanospindles with widths of about 30–60 nm and lengths of about 80–150 nm are formed. The irregular diffraction rings are observed from the SAED pattern of the obtained sample (Fig. 1d). However, it can be determined that the obtained sample is the crystalline structure.

To further reveal the microstructures of the sample, the Raman spectra and high-resolution TEM images are given in Fig. 2. In the Raman spectra, two dominant Raman shifts at about 1350 and 1590 cm^{-1} are observed, respectively. [12] The peak at about

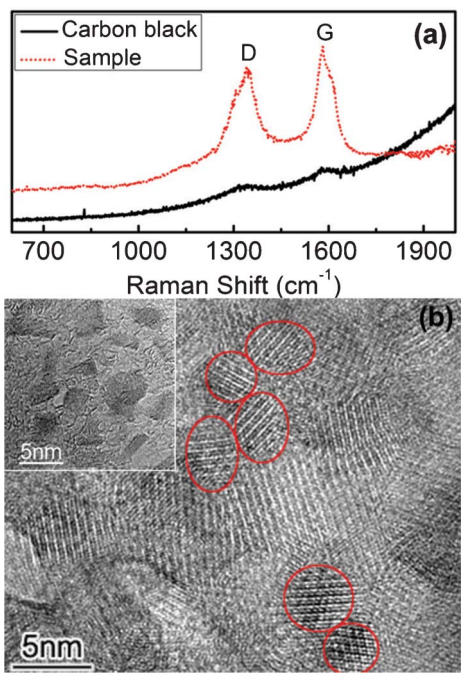

Fig. 2 (a) Raman spectra of carbon black nanoparticles and carbon nanospindles, respectively. (b) HRTEM images of carbon nanospindles, the inset is the HRTEM image of some carbon nanocrystals with a variety of shapes accompanying shuttle-like nanostructures.

1590 cm^{-1} is associated with the well-known E_{2g} vibrational model of sp^2-bonded carbon atoms in the graphene layers, *i.e.*, G band. The peak at 1350 cm^{-1} (D band) is identified with symmetry-forbidden modes associated with the maximum in the graphite density of states, activated by lattice disorder and/or small crystalline size.[19] Two such dominant Raman peaks of the sample are much stronger than those of carbon black particles, suggesting the differences of the microstructures between the sample and carbon black. The direct observation for the sample is obtained by HRTEM images. It can be seen that carbon nanospindle is composed of many small carbon nanocrystals. Some distinct carbon nanocrystals are labelled in Fig. 2b by red circles. Therefore, the interfaces between carbon nanocrystals act as defects, resulting in the appearance of the strong and broadened D bands. In addition, the G band is broadened, indicating a polycrystal microstructure with some defects.

Furthermore, some carbon nanocrystals alone are observed and assume various shapes (the inset of Fig. 2b). However, most of the carbon nanocrystals obtained at the short pulse width were spherical. With the increase of pulse width, large carbon nanoparticles composed of a few of small carbon nanocrystals were obtained.[8] These results suggest that the carbon nanospindle could be formed by coalescence of small carbon nanocrystals. The possible mechanism is described in Scheme 1. The pulse width for the formation of carbon nanospindles is 10–20 times longer than that for the formation of only small nanoparticles (Scheme 1a). According to previous studies, the spindle-like bubbles contained carbon clusters in the liquid are immediately formed after laser ablation of the carbon black suspension (S1 of Scheme 1b).[8–10] When the temperature of the spindle-like bubbles starts to drop down from the peak value, the condensation of carbon clusters takes place along the boundary of the spindle-like bubble due to preferential cooling or higher cooling rates,[3,4] resulting in the formation of small carbon nanocrystals (S2 of Scheme 1b).[7] With the generation of more and more carbon nanocrystals, the first layer of carbon nanocrystals is formed along the boundary of the spindle-like bubble and then new carbon nanocrystals nucleate at the place of the adjacent layer (S3 of Scheme 1b).[3,4] By analogy, carbon nanospindles are obtained finally (S4 of Scheme 1b). On

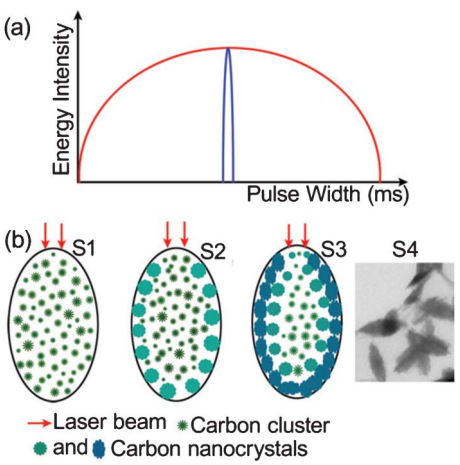

Scheme 1 (a) Relationships between laser pulse widths and pulse energy intensity; (b) Illustrations of the formation of carbon nanospindles by assembly of carbon nanocrystals.

the basis of the experiment results, it is decisive for the coalescence of small carbon nanocrystals that enough time and energy are possibly provided at the long pulse width. However, the bubbles could collapse at the short pulse width due to quickly heating up and cooling down, only forming dispersed carbon nanoparticles.

The OL responses of the obtained sample are shown in Fig. 3a, in which the output fluence was plotted as a function of input fluence. The OL curves were directly converted from the Z-scan spectra. The OL responses of carbon black suspension toward 6 ns laser pulses at 532 nm were determined as references, where the suspension of 81% linear transmittance was obtained from commercial india ink *vis* dilution with water. As shown in Fig. 3a, the OL reaches a plateau at a threshold input fluence of about 0.7 J cm^{-2} and the saturated output fluence at the plateau is 0.26 J cm^{-2}. A stable suspension of carbon nanospindles was prepared *via* sonication in the water, and then diluted with the addition of an appropriate amount of water so that the linear transmittance of the suspension was 81% at 532 nm. As shown in Fig. 3a, the carbon nanospindle suspension limits nanosecond laser pulses significantly, with the saturated output fluence of about 0.15 J cm^{-2} at the plateau, which is much below that for the carbon black suspension. Therefore, the OL effects from the carbon nanospindle suspension are much better than that from the carbon black suspension at the same linear transmittance. The OL properties can be quantitatively compared by the OL threshold (defined as the input fluences at which the transmittance falls to 50% of the normalized linear transmittance).[13] It can be seen from Fig. 3b that the OL thresholds of the sample and carbon black are about 0.14 and 0.37 J cm^{-2}, respectively. This also suggests that the obtained sample shows a better OL response.

The optical limiting effects are attributed to two main mechanisms: NLS and nonlinear absorption.[11–15] According to different materials and absorption mechanisms, the latter is divided into multiphoton absorption, reverse saturable absorption, and FCA.[12] The generally accepted underlying OL mechanism for the suspensions of carbon black, carbon nanotubes and graphene nanosheets is dominated by NLS, [11–14] whereas for small nanoparticle suspension it is two photon and/or multi-photon

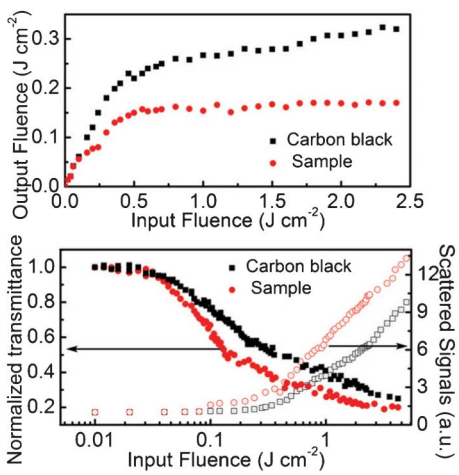

Fig. 3 The OL responses of carbon black and shuttle-like carbon nanostructure suspensions for 6 ns pulsed laser at 532 nm. (a) Output fluence *vs.* input fluence. (b) Nonlinear transmittance and scattering spectra *vs.* input fluence.

absorption for pico-femtosecond laser pulses and FCA and/or NLS for nanosecond laser pulses.[15–17] To elucidate the OL mechanism, the NLS behaviour of the sample was measured and is shown in Fig. 3b. In our experiment, strong light scattering was observed when the suspensions passed through the focus of the incident beam. We collect a fraction of scattered light using a convex lens at 45° horizontal to the direct incident beam. In the scattering process, the high-energy laser beam is dispersed to have large spatial dimensions and so the achievement of the reduced intensity. It can be seen from Fig. 3b that the scattered intensities increase along with the decrease of the transmittance, indicating that the NLS is responsible for the OL. We noticed that the growth rate of scattered signals from the sample is faster than that from carbon black suspension toward the 6 ns laser pulsed at 532 nm. Moreover, the onset of the growth of scattered signals is synchronous with the onset of the decrease of transmittance for the sample.

According to Mie theory, the scattering efficiency Q_{sca} can be expressed as

$$Q_{sca} = \frac{2}{X^2}\sum_{n=1}^{\infty}(2n+1)\left(|a_n|^2+|b_n|^2\right) \quad (1)$$

where $X = 2\pi r/\lambda$, r and λ are the particle radius and the incident laser wavelength, respectively. The coefficients a_n and b_n represent the magnetic and electric multipoles of order n, respectively. Based on the above equation (1), the scattering efficiency is related to the particle size and laser wavelength. The effective scattering arises from the particles with size on the order of the wavelength of the incident laser beam.[12] In our experiment, the incident laser wavelength of 532 nm is far larger than the size of the carbon nanospindles. Accordingly, a light beam cannot be effectively scattered by nanoscale particles alone. Referring to the optical limiting mechanism for carbon black, the effective scattering centers possibly originate from the generation of the bubbles on the solid/liquid interfaces. The carbon nanospindles are heated by the incident laser and then could be ionized. Thus, the bubbles are formed and expand quickly due to the large pressure difference at the vapor-liquid interface. When the size of bubbles grows to the magnitude of the incident laser wavelength, the bubbles effectively scatter the incident beam, realizing the reduction of transmission. The dynamics of the expansion or collapse process of a spherical bubble can be described by the Rayleigh–Plesset equation[12]

$$\rho\left[r\frac{d^2t}{dt^2}+\frac{3}{2}\left(\frac{dr}{dt}\right)^2+\frac{4v}{r}\frac{dr}{dt}\right] = P(t)-P_\infty(t)-\frac{2\gamma}{r} \quad (2)$$

where ρ, γ and v are density, surface tension and kinematic viscosity of the liquid, respectively. P and P_∞ are the pressures inside the bubble and far from the bubble, respectively. Since carbon black particles and carbon nanospindles are dispersed in the water, ρ, γ and v are constant and thus the dynamics of the expansion or collapse process of the bubble depends on P, which is associated with the laser energy absorption of the carbon suspension. However, there are possible effects of the size and structure of carbon particles on the laser energy absorption of the carbon suspension. Hence, the suspensions of carbon black particles and carbon nanospindles exhibit different OL responses.

In conclusion, carbon nanospindles from the coalescence of small carbon nanocrystals were prepared by laser ablation of a carbon black suspension. Their formation requires the long pulse width that can provide enough time and energy for coalescence of small nanocrystals. Moreover, carbon nanospindles exhibit excellent OL responses, which are promising in nonlinear optical devices.

This work is financially supported by the National Natural Science Foundation of China (Nos. 50902126, 51172214), Shanxi Province Science Foundation for Youths (No. 2009021027), and Program for the Top Young Academic Leaders of Higher Learning Institutions of Shanxi.

References

1 K. Y. Niu, J. Yang, S. A. Kulinich, J. Sun, H. Li and X. W. Du, *J. Am. Chem. Soc.*, 2010, **132**, 9814.
2 P. Liu, H. Cui, C. X. Wang and G. W. Yang, *Phys. Chem. Chem. Phys.*, 2010, **12**, 3942.
3 Z. Yan, R. Bao, Y. Huang, A. N. Caruso, S. B. Qadri, C. Z. Dinu and D. B. Chrisey, *J. Phys. Chem. C*, 2010, **114**, 3869.
4 Z. Yan, R. Bao and D. B. Chrisey, *Nanotechnology*, 2010, **21**, 145609.
5 S. C. Singh, S. K. Mishra, R. K. Srivastava and R. Gopal, *J. Phys. Chem. C*, 2010, **114**, 17374.
6 P. Liu, Y. Liang, X. Lin, C. X. Wang and G. W. Yang, *ACS Nano*, 2011, **5**, 4748.
7 G. W. Yang, *Prog. Mater. Sci.*, 2007, **52**, 648.
8 S. Hu, J. Liu, J. Yang, Y. Wang and S. Cao, *J. Nanopart. Res.*, 2011, **13**, 7247.
9 S. Hu, K. Y. Niu, J. Sun, J. Yang, N. Zhao and X. W. Du, *J. Mater. Chem.*, 2009, **19**, 484.
10 S. Hu, F. Tian, P. Bai, S. Cao, J. Sun and J. Yang, *Mater. Sci. Eng., B*, 2009, **157**, 11.
11 J. E. Riggs, D. B. Walker, D. L. Carroll and Y.-P. Sun, *J. Phys. Chem. B*, 2000, **104**, 7071.
12 J. Wang, Y. Hernandez, M. Lotya, J. N. Coleman and W. J. Blau, *Adv. Mater.*, 2009, **21**, 2430.
13 Y. Gao, Y. S. Zhou, J. B. Park, H. Wang, X. N. He, H. F. Luo, L. Jiang and Y. F. Lu, *Nanotechnology*, 2011, **22**, 165604.
14 J. Wang and W. J. Blau, *J. Phys. Chem. C*, 2008, **112**, 2298.
15 Y.-P. Sun, J. E. Riggs, H. W. Rollins and R. Guduru, *J. Phys. Chem. B*, 1999, **103**, 77.
16 W. Jia, E. P. Douglas, F. Guo and W. Sun, *Appl. Phys. Lett.*, 2004, **85**, 6326.
17 G. Wang and W. Sun, *J. Phys. Chem. B*, 2006, **110**, 20901.
18 S. N. Baker and G. A. Baker, *Angew. Chem., Int. Ed.*, 2010, **49**, 6726.
19 V. Z. Mordkovich, *Chem. Mater.*, 2000, **12**, 2813.

